Journal of Power Sources 195 (2010) 3922–3927

Contents lists available at ScienceDirect

Journal of Power Sources

journal homepage: www.elsevier.com/locate/jpowsour

Short communication

Cathode material influence on the power capability and utilizable capacity of next generation lithium-ion batteries

Michael A. Roscher[a,*], Jens Vetter[b], Dirk Uwe Sauer[a]

[a] RWTH Aachen University, Electrochemical Energy Conversion and Storage Systems Group, Institute for Power Electronics and Electrical Drives (ISEA), 52066 Aachen, Germany
[b] BMW Group, 80788 München, Germany

ARTICLE INFO

Article history:
Received 23 June 2009
Received in revised form 29 October 2009
Accepted 27 November 2009
Available online 6 January 2010

Keywords:
Li-ion
Olivine cathode
Pulse power
Available capacity
Load history

ABSTRACT

Lithium-ion cells (Li-ion) comprising lithium iron phosphate ($LiFePO_4$) based cathode active material are a promising battery technology for future automotive applications and consumer electronics in terms of safety, cycle and calendar lifetime and cost. Those cells comprise flat open circuit voltage (OCV) characteristics and long-term load history dependent cell impedance. In this work the special electric characteristics of $LiFePO_4$ based cells are elucidated, quantified and compared to Li-ion cells containing a competing cathode technology. Through pulse tests and partial cycle tests, performed with various olivine based cells, the cycling history dependency of the internal resistance and therefore on the power capability is shown. Hence, methods are illustrated to quantify this load history impact on the cells performance. Subsequently, methods to achieve a safe battery operation are elucidated. Furthermore strategies are given to obtain reliable information about the cells power capability, taking the mentioned properties into consideration.

1. Introduction

In the course of investigations on new electrode materials for lithium-ion batteries (Li-ion) the iron based olivine type cathodes (mainly lithium iron phosphate, $LiFePO_4$) were identified as possible alternatives to cathodes based on rare metal composites (i.e. the transition metal oxides $LiCoO_2$, $LiNiO_2$) [1,2]. Besides the resulting positive cost factor such cathodes are intrinsically safe and show a very good cycle life [3]. Hence, Li-ion cells based on olivine cathode materials will be a promising technology for safety sensitive and low-budget mass products e.g. hybrid electric vehicles (HEV) and battery electric vehicles (BEV). However, cells containing these olivine cathodes have a reduced nominal voltage in comparison to competing Li-ion cells and thus have a slightly reduced energy density. Additionally, it is known that these cells show very special electrical properties according to their open circuit voltage (OCV) characteristics.

The certain processes within the $LiFePO_4$ leading to this specific OCV effects will be elucidated. Subsequently, the impact of these special processes on the pulse power and partial cycle characteristics is investigated and compared to cells containing metal oxide cathodes.

2. Theoretical background

2.1. Two-phase transition of active electrode materials

Among other active materials for Li-ion cells (e.g. lithium cobalt oxide $LiCoO_2$, lithium nickel oxide $LiNiO_2$, lithiated graphite LiC_6) the lithium iron phosphate shows a special kind of lithium insertion/extraction process. The insertion or extraction, respectively, proceeds via a first order phase transition [4]. During lithium (Li) insertion into a cathode particle (discharge) the particles surface region becomes lithiated and two distinct phase regions (a lithiated phase and a delithiated phase region) emerge within the originally homogenous material. Between the two regions a phase barrier exists. One phase is transformed into its particular counterpart as Li insertion proceeds and the barrier propagates from the particles surface towards the center. The lithium concentrations within each phase region remains constant. This two-phase transition continues until the particle is completely transformed.

Analogously, during lithium de-insertion the particles surface region becomes delithiated first and the phase barrier propagates towards the particles center again until the particle is completely delithiated.

The phase separation in the two-phase state is stable over time. Hence, the phase barrier does not vanish through diffusion processes during longer rest periods.

Levi et al. relate the existence of the two-phase transition to strong attractions between the host lattice (i.e. $FePO_4$) and the lithium (guest). These attractions avoid the composition of

* Corresponding author. Tel.: +49 89 38211380; fax: +49 89 3827011380.
E-mail address: michael.roscher@rwth-aachen.de (M.A. Roscher).

0378-7753/$ – see front matter © 2009 Elsevier B.V. All rights reserved.
doi:10.1016/j.jpowsour.2009.11.143

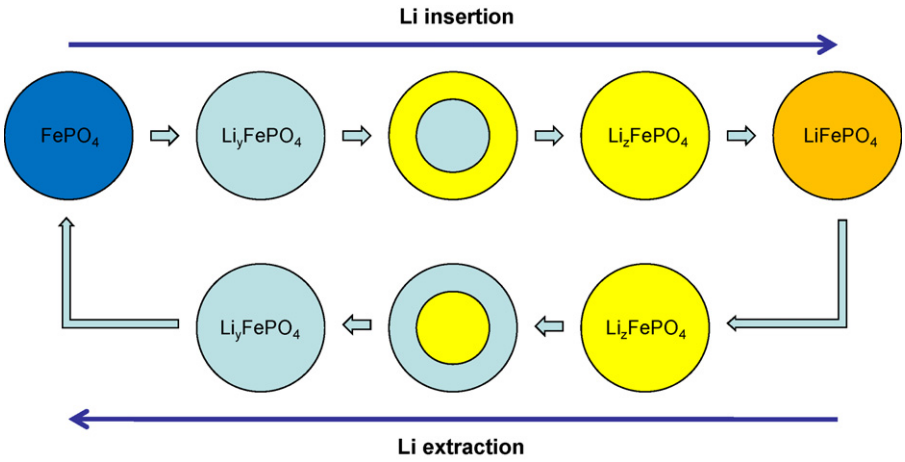

Fig. 1. Complete Li insertion and de-insertion cycle of a spherical $LiFePO_4$ particle.

homogenous phases in certain ranges of lithium content $0 \leq x \leq 1$ in Li_xFePO_4 [5].

Certain Li contents are energetic favorable states for the host lattice (minima of free energy) [6]. Li contents between two favorable states cannot exist and separated phase regions emerge as a consequence. The distinct Li contents x of the energetic minima depend on the temperature [5] and the particle size [4]. In Li_xFePO_4 two energetic favorable contents x exist in the possible range $0 \leq x \leq 1$. Between these two Li contents the lithium insertion proceeds as a two-phase transition.

Srinivasan and Newman report a content range of $0.02 < x < 0.9525$ [7] and Gaberscek et al. relate the two-phase transition to the range of $0.05 < x < 0.89$ [8], in contrast.

In spite of the different data mentioned, it can be assumed that the Li insertion and de-insertion in Li_xFePO_4 mainly occurs via two-phase transition. For very low ($x \to 0$) and very high Li contents ($x \to 1$) the Li insertion/extraction homogenously proceeds as a solid state reaction [7].

A comprehensive Li insertion and extraction process of a spherical particle is schematically depicted in Fig. 1, where the index y is related to the first energetic minimum and z to the second minimum during the transition of $FePO_4$ to $LiFePO_4$. As mentioned above, the phase sequence during Li insertion differs from the sequence while the de-insertion occurs. During insertion an expanding lithiated shell surrounds a delithiated core. Respectively, a lithiated core is enclosed by a delithiated shell during Li de-insertion.

2.2. Impact of the two-phase transition on the OCV characteristics

During the two-phase transition the electrode potential shows pronounced voltage plateaus due to the constant lithium concentrations within the phase regions. The surface region is lithiated during the whole insertion process. The incoming lithium leads only to a shift of the phase barrier. Hence, the electrode potential being associated to the Li concentration within the particles outermost phase regions remains constant. Analogously, the surface region is delithiated during Li de-insertion.

Therefore, the OCV curves of Li-ion cells based on a graphite anode and a $LiFePO_4$ containing cathode are very flat since $LiFePO_4$ as well as graphite show a two-phase transition behavior during Li insertion and de-insertion. In SOC ranges in which both of the involved active materials perform a two-phase transition the OCV curves comprise gradients less than 1 mV/% ΔSOC (SOC = 30–60% and SOC = 70–90%) [9].

Fig. 2 gives an illustration of the differences between the OCV curves of a metal oxide and a $LiFePO_4$ based cell (each comprising graphite anode). The OCV's are plotted versus the state-of-charge (SOC), normalized to the nominal capacity (completely charged cell → SOC = 100%). The OCV of the metal oxide cell increases by 0.6 V nearly linear from SOC = 0–100%. As visible, the OCV of the olivine cell shows only slight changes with varying SOC. In the SOC boundary regions the OCV gradient increases (SOC → 0%, SOC → 100%, respectively). Additionally, the OCV exhibits a kind of voltage hysteresis. Such hysteresis phenomena are well known from NiMH batteries [10] and were also documented for Li-ion cells in [9].

2.3. Impact of the two-phase transition on the internal resistance

The development of separated phase regions within the particles of electrode materials affects the electrical performance of Li-ion cells. If the outermost phase region is lithiated the lithium can directly be extracted from the surface region during Li de-insertion. In the case of a delithiated shell phase (and a lithiated core) the lithium has to overbear the distance from the lithiated core to the particles surface during de-insertion, even if the stoichiometric lithium concentration might be equal to the previous case.

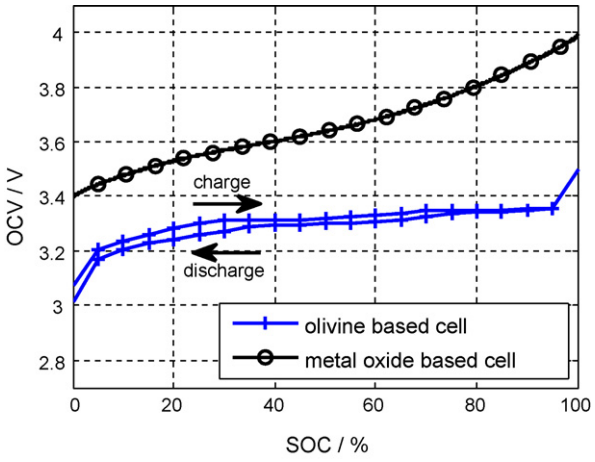

Fig. 2. OCV of olivine based ($LiFePO_4$) and metal oxide based cells (3 h rest period at each SOC step).

Analogously, the Li can be inserted into the host lattice at the particles surface if the outermost phase region is delithiated. Otherwise the lithium has to cover the distance through the shell region to the phase barrier to get inserted to the lattice.

The movement of the lithium within the active material causes a measurable diffusive voltage drop during load of a Li-ion cell and therefore determines the cells internal resistance [3,11]. Hence, the cell internal resistance depends on the load history due to the development of various phase region sequences within the active particles. A qualitative overview to the impact of the phase region development on the electrical characteristics of $LiFePO_4$ based Li-ion cells is given in [11].

Comparative results (pulse and cycle tests) of cells comprising olivine and metal oxide cathodes will be given and discussed in the following sections.

3. Experimental

To get comprehensive information about the influence of the load history on the electrical characteristics two different types of $LiFePO_4$ olivine based cells are tested (high power prototype cells and high energy cells, both types sourced from different manufacturers). To outline the different behaviors of cells containing various cathode materials a metal oxide based high energy cell type is tested, too.

The tests are done on a Scienlab test bench. The cell voltages and currents are measured with a 24 bit analog–digital-converters (accuracy: 0.25% of the measured value ±1 mV) and LEM current sensors (accuracy: 0.25% of the measured value ±30 mA in a range of −30 A to 30 A and 0.25% of the measured value ±600 mA for higher currents, respectively), integrated to the test bench. During testing the cells are located in a CTS climate chamber and the temperatures are detected with NiCr–Ni thermal couples (temperature resolution and accuracy: ±1 K). The couples are pasted to the cells cases.

In a first test the power capability of the three different cell types and especially the influence of the load history on the pulse power are investigated. Therefore, constant voltage (CV) pulses are applied to the cells for 20 s at various SOC values (SOC = 20%, 40%, 60%, 80%). Prior to the tests the cells were charged to SOC = 100% with a CCCV (constant current, constant voltage) charge regime (charging until the cutoff voltage is reached (olivine cells: 3.6 V with 1 C-Rate (C); metal oxide cells: 4.2 V, 0.2 C) and subsequently charged with cutoff voltage for 30 min). Then the cells were discharged to SOC = 80% (CC-discharge). After 30 min pause time the 20 s CV pulse is applied and the cells are discharged to SOC = 60% and so forth. After the pulse test at SOC = 20% the cells were completely discharged and subsequently charged to SOC = 20% again. Thereafter a rest period (30 min) followed by the next pulse is applied and the cells are charged to SOC = 40% and so on. During the first test loop only discharge pulses are performed. The comprehensive test is repeated performing charge pulses only. Thus, current profiles (CV discharge and CV charge pulses) are obtained for SOC = 20%, 40%, 60%, 80% after the SOC being adjusted through discharge and charge, as well.

The cutoff voltages during the CV pulse periods were chosen as follows:

- olivine power cells: 3.7 V charge/2.6 V discharge
- olivine energy cells: 3.8 V charge/2.2 V discharge
- metal oxide cells: 4.2 V charge/2.5 V discharge

The voltage limits for the power cells were chosen more conservative in order to prevent currents exceeding the allowed current limits specified by the manufacturer.

The partial cycle tests are performed with the two different olivine based cells. After CCCV charge an SOC = 50% is adjusted through CC-discharge (power cells: 1 C, energy cells: 0.2 C, SOC sequence: 100% → 50%). After 30 min rest period the cells are discharged with various current rates until the cell voltages reach 2.5 V. After a next CCCV charge and adjustment to SOC = 50% the cells are charged (CC, various C-Rates) until the charge cutoff voltage (3.6 V) is hit. Then the cells get CCCV charged, 100% of the nominal capacity (C_n) is taken out of the cells and after that they are charged to SOC = 50% (SOC sequence: 0% → 50%). Subsequently, the cells are discharged (CC) until 2.5 V. Past to a next adjustment cycle (CCCV, 100% C_n extraction, charge to SOC = 50%) the cells are charged (CC) to 3.6 V.

The current rates of the final load periods are chosen to:

- olivine power cells: 1 C, 3 C, 10 C
- olivine energy cells: 0.3 C, 0.5 C

All experiments are accomplished at a constant temperature of the climate chamber (25 °C).

4. Results

4.1. Charge history dependent power capability

The performed pulse power test at various SOC values with varied load history (from complete charged state as well as from the complete discharged state) revealed significant differences in the power capability of $LiFePO_4$ based cell according the SOC adjustment regime. To outline the specific behaviors Fig. 3 gives typical current profiles (charge pulses Fig. 3a, c, e and discharge pulses Fig. 3b, d, f) during testing of the investigated cells after SOC adjustment through charge (denoted as: after charge) and discharge (denoted as: after discharge), respectively, with the currents being normalized to the cells nominal capacity rate (C-Rate). According to the constant voltages during the pulses the current values are proportional to the cell power values. The specific initial SOC values were 20%, 40%, 60%, 80%, as mentioned above.

As visible in the shown diagrams, for the high energy olivine cells (Fig. 3c and d) the available power strongly depends on the way the SOC is reached. After charging the discharge current is nearly independent from SOC. After discharge the discharge currents significantly differ. This behavior cannot be assigned to the OCV hysteresis alone. In a rough calculation for the shown case (Fig. 3d): 2.2 V constant voltage discharge of an olivine energy cell at SOC = 20%, the OCV prior to the pulse is 3.35 V after charge and 3.3 V after discharge. Hence, the voltage reserves to the cutoff voltage differ less than 5% (1.15 V ↔ 1.1 V). However, the measured currents differ more than 30% at the end of the pulse. This indicates a changed internal resistance superimposing the OCV hysteresis effect and having a much stronger impact on the power capability. The measurement results show that the path dependence of the pulse current capability of olivine based cells increases as the SOC reaches the boundary regions (very high, very low SOC). The charge power differs at high SOC values stronger than at low SOC values, whether the SOC is adjusted through charge or discharge. Analogously, the discharge power at low SOC values depends stronger on the SOC adjustment, in comparison to tests at higher SOC values.

The available power of the metal oxide cells (Fig. 3e and f) is quite independent from the charge history but is closely correlated to the SOC, in contrast. Hence, the power capability decrease goes hand in hand with the decreasing voltage reserve, due to the changing OCV.

The power pulse results of the power cells are a mixture of SOC and load history dependency. Even though, the power capabil-

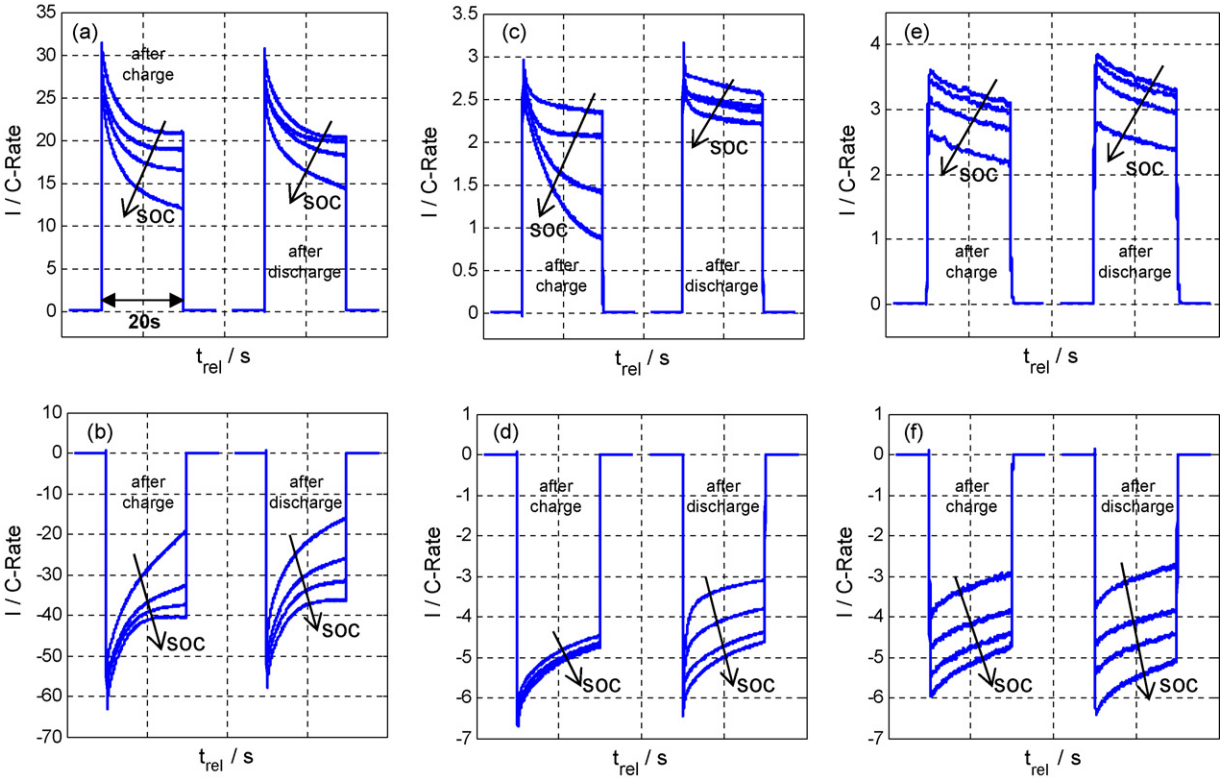

Fig. 3. Typical current profiles during CV charge and discharge pulse testing at SOC = 20%, 40%, 60%, 80% of olivine power cells (a, b), olivine energy cells (c, d) and metal oxide energy cells (e, f) after charge and discharge initial SOC adjustment.

ity differs approximately 10%, whether the initial SOC is adjusted through charge or discharge, there is a noticeable difference in the power values for various initial SOC values (independent from SOC adjustment direction). We presume this fact to be related to the large amount of charge throughput during one pulse (ten times higher ΔSOC in comparison to the energy cells) and the dedicated change in the OCV and ion depletion effects in the active materials and within the electrolyte.

Just at the beginning of each of the pulses the power capability is nearly independent from SOC and SOC adjustment for both of the investigated olivine cell types. Rather the differences noticeably emerge during ongoing pulse duration, which is not the case for the metal oxide cells. Thus, at the beginning of the pulses the current is sourced from the electric double layer capacity of the electrodes and after that the different resistances of the active materials come into play.

4.2. Charge history dependent available discharge capacity

If the internal resistance varies according to the SOC adjustment, also an influence on the available capacity is assumed, due to the cutoff voltage value during charge/discharge cycling is expected to be reached earlier or even later, respectively. Fig. 4a gives the typical cell voltage of the energy cells during a 0.3 C discharge. The initial SOC = 50% firstly was adjusted through discharging completely charged cells and secondly through charging of an empty cells. The discharge current stops as a voltage of 2.5 V is reached. The differences between the two curves are obvious, indicating different internal resistances of the same cell, originating from the way the SOC was adjusted only. Hence, it is evident that the load history has a strong impact on the short time internal resistance (pulse tests in Section 4.1) as well as on the long-term resistance.

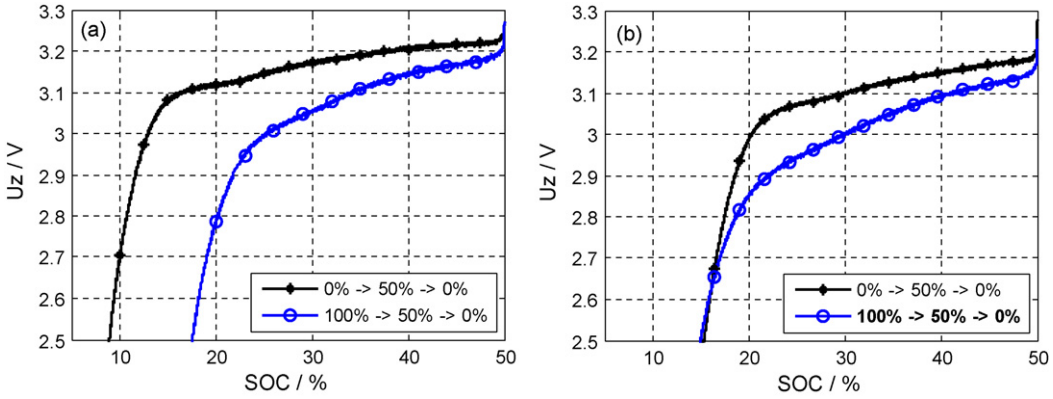

Fig. 4. Voltage profiles during discharge of prismatic olivine based cells (left: 0.3 C-rate current; right: 0.5 C-rate current) plotted vs. SOC, depending on the load history.

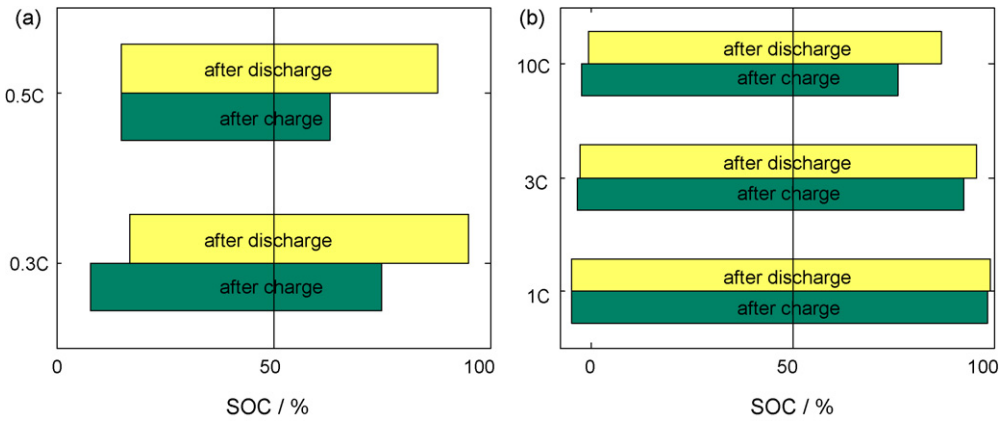

Fig. 5. Typical SOC values when the cutoff voltages are reached at various current rates of $LiFePO_4$ based energy cells (a) and power cells (b), depending on the SOC adjustment direction, starting at SOC = 50%.

Fig. 4b gives the voltages during the same tests, but with a discharge rate of 0.5 C. During most time of the discharge period the differences between the curves are similar to the ones obtained during the 0.3 C discharge period. As the voltages are decreasing due to the decreasing OCV in this range, the voltage gap between the curves decreases, too. In our opinion, this effect correlates to the difference in the internal power losses resulting in an unequal self heating of the cells. Actually, the measured cell temperatures at the end of each 0.5 C test differ approximately 7 K. The self heating leads to an enhanced conductivity of the active materials. Hence, the overvoltage decreases, subsequently the available capacity increases. Surprisingly, this leads to a higher usable discharge capacity for a 0.5 C discharge compared to 0.3 C discharge rate, if the SOC = 50% is adjusted by discharging of a completely charged olivine based energy cell.

Fig. 5 gives a quantitative illustration of the available charge and discharge capacities of olivine based cells starting at a SOC of 50% (at room temperature). The given percentages are the SOC values of the cells as they are reaching the distinct cutoff voltages.

For the energy cells the SOC history dependency is much stronger than for the power cells.

5. Discussion

5.1. Consequences in applications

The earlier sections gave a qualitative and quantitative overview in which way the charge/discharge history, especially the SOC adjustment sequence, influences the power capability and available capacity of olivine based cells. Therefore, the results outlined in Sections 4.1 and 4.2 compare the best to the worst possible load cases for cells in an application. Fortunately, these artificial test cases, including full charge and complete discharge, are not typical operating conditions for i.e. automotive applications. In hybrid electric vehicles (HEV) systems the operation windows would be defined much smaller (e.g. SOC = 30–60%), according to power requirements, cold cranking and aging issues. In battery electric vehicles (BEV) applications the operation window may be extended to SOC = 0–100%, but the cells are mainly discharged during drive cycles. This means, an SOC of 80% is seldom reached through regeneration starting form SOC = 0%, for example. During the charge phases (i.e. connected to grid for several hours) the power and capacity differences caused by changed internal resistances can be neglected, due to the long charge periods.

However, during full cycle tests or typical parameterization test schedules (FreedomCAR [12], HPPC from the PNGV [13]) the cells undergo the best or the worst load case, respectively. Hence, if the results from such tests are used for power prediction jobs in battery management systems, in most cases the available power will be under- or even overestimated. Underestimation is not critical. The storage system is always able to supply the predicted power, but this would reduce the systems utilization. Overestimation can result in hitting or exceeding the cells voltage and/or current limits during a power controlled load section. This may lead to dangerous storage temperatures, a reduced calendar life or to an irreversible damage of the entire storage system.

5.2. Power prediction approaches

As a simple method to prevent any dangerous battery states caused by a wrong power prediction would be the introduction of voltage and current buffers to reduce the usable operation window of the cells, hence, to prevent the exceeding of the limits, even if the predicted power is applied to or taken from the battery system. Due to the results from pulse tests in Section 4.1 the buffers have to be dimensioned carefully. If the buffers are dimensioned in a way that the cell limits are not violated, even in the SOC boundary regions, the power capability utilization would be reduced about 30–50% over the entire SOC range.

Another method would be a conservative parameterization. All set points for power maps are carried out by worst case measurements (charge tests after charge dominant SOC adjustment and discharge tests after discharge dominant SOC adjustment, respectively). In contrast to the method outlined before, the system utilization would be better in the mid SOC region, but in most cases the predicted power is significantly lower than the power the storage system can actually supply. This would still not be tolerable for high power applications like HEV systems.

As mentioned in Section 4.1 the power capability of olivine cells for very short-term pulse durations is nearly independent from SOC and SOC history. Hence, these two parameters can be neglected for the prediction very short-termed power capability.

If a rigorous prediction over longer terms is required, the SOC as well as the load history has to be taken into account when predicting power and available energy. The best and the worst use cases have to be mentioned in a kind of histogram considering the SOC sequence since the last complete charging or discharging, respectively. From such data the cells actual state can be derived, continuously shifting between the best and the worst use case. According to that, the instantaneous cell impedance shifts between its minimum and maximum value. For charge the impedance differs from the discharge impedance. For this purpose the usage of a SOC sequence memory stack, as it is presented in [11] is appropriate. This approach also considers the transition from a low to a high

impedance state. The power prediction itself can be done based on a typical batteries equivalent electric circuit using the OCV, the electrical cell limits (cutoff voltages, current limits) and the batteries impedance [14].

Besides a model based power prognosis approach, the usage of fuzzy logic systems or artificial neural networks incorporating, e.g. the OCV, the cell limits, and the information about the SOC sequence are possible solutions, but will need further investigations on this topic.

5.3. Parameterization test schedule for comprehensive cell characterization

It is evident that the strong SOC sequence influence on the power characteristic of olivine based cells makes necessary to carry out power results for both the best and the worst cases. That means discharge tests have to be done after the cells were discharged and after the cells were charged, too (analogously for the charge tests). A possible procedure for pulse tests would be as follows:

1. CCCV
2. SOC adjustment (discharge)
3. discharge pulse
4. rest period
5. charge pulse
   (repeat steps 2–5 until SOC_{min})
6. SOC adjustment (charge)
7. charge pulse
8. rest period
9. discharge pulse
   (repeat steps 6–9 until SOC_{max})

Test steps 3 and 7 are the worst case and steps 5 and 9 are the best case tests. This measurement is rigorous only if the SOC change during one pulse section can be neglected. Otherwise charge and discharge tests cannot be carried out during the same test. Hence, it is obvious that a comprehensive pulse power characterization (over the complete temperature range and with different currents) alone needs a multiple of the time, compared to the HPPC or FreedomCAR tests. Furthermore, capacity tests are more complex, due to the initial SOC having a strong impact on the capacity reserve under constant current condition. Partial cycle tests are required and tests to determine the transition from a low resistive to a higher resistive case (the way around is not possible) are mandatory to obtain a comprehensive electrical characterization.

6. Conclusion

In this work the power capability of Li-ion cells, including $LiFePO_4$ based cathodes, at different initial SOC was investigated and compared to metal oxide based cells. The olivine based cells show a strong impact of the way the initial SOC was adjusted (not the SOC itself) on the power capability, in contrast to the metal oxide based reference cells. The charge power capability is much higher after the initial SOC being adjusted through discharge than after a charge SOC adjustment. Analogously, the discharge power is higher after charge than after discharge. The SOC itself is less relevant.

Subsequently, a strong influence of the SOC adjustment regime on the available capacity is identified. As expected from the power tests, the charge capacity is higher after discharge dominated SOC adjustment and vice versa. According to the obtained results a number of applicable concepts for the development of online power prediction algorithms are outlined. A simple test schedule is introduced considering the need for a detailed characterization of the mentioned effects.

The aim of this work was to show that olivine based cells (mainly $LiFePO_4$ based cells) offer a number of challenges related to the development of reliable management strategies, beside the apparent advantages this technology offers in comparison to competing Li-ion technologies. It was shown that the typical and wide spread power and capacity test schedules would not generate all of the results, which would be necessary in order to obtain a comprehensive cell characterization.

References

[1] J.B. Goodenough, A.K. Padhi, K.S. Nanjundaswamy, C. Masquelier, US Patent 5,910,382 (1999).
[2] A.K. Padhi, K.S. Nanjundaswamy, J.B. Goodenough, J. Electrochem. Soc. 144 (1997) 1188–1194.
[3] K. Striebel, J. Shim, V. Srinivasan, J. Newman, Lawrence Berkley National Laboratory, Paper LBNL55781, 2004.
[4] N. Meethong, H.-Y. Shadow Huang, W.C. Carter, Y.-M. Chiang, Electrochem. Solid State Lett. 10 (2007) 134–138.
[5] M.D. Levi, D. Aurbach, Electrochim. Acta 45 (1999) 167–185.
[6] N. Meethong, H.-Y. Shadow Huang, S.A. Speakman, W.C. Carter, Y.-M. Chiang, Adv. Funct. Mater. 17 (2007) 1115–1123.
[7] V. Srinivasan, J. Newman, J. Electrochem. Soc. 151 (2004) 1517–1529.
[8] M. Gaberscek, R. Dominko, J. Jamnik, J. Power Sources 174 (2008) 944–948.
[9] J. Gerschler, D.U. Sauer, Investigation of Open-Circuit-Voltage Behavior of Lithium-Ion Batteries with Various Cathode Materials under Special Consideration of Equilibrium Voltage Phenomena, Elec. Vehicle Symp. 24 (2009).
[10] V. Srinivasan, J.W. Weidner, J. Newman, J. Electrochem. Soc. 148 (2001) 969–980.
[11] M.A. Roscher, J. Vetter, D.U. Sauer, J. Power Sources 191 (2009) 582–590.
[12] U.S. Department of Energy, FreedomCAR Battery Test Manual For Power-Assist Hybrid Electric Vehicles, DOE/ID-11069, 2003.
[13] U.S. Department of Energy, PNGV Battery Test Manual, Rev. 0, DOE/ID-10597, 1997.
[14] G. Plett, International Patent WO 2005/050810 A1 (2004).